Eur Food Res Technol (2015) 240:109–118
DOI 10.1007/s00217-014-2312-y

ORIGINAL PAPER

Binding of a novel bacteriostatic agent—chitosan oligosaccharides–kojic acid graft copolymer to bovine serum albumin: spectroscopic and conformation investigations

Xiaoli Liu · Wenshui Xia · Qixing Jiang · Yanshun Xu · Peipei Yu

Received: 5 June 2014 / Revised: 30 July 2014 / Accepted: 9 August 2014 / Published online: 2 September 2014

Abstract In this paper, a novel chitosan oligosaccharides derivative—chitosan oligosaccharides–kojic acid graft copolymer (COS/KA), COS, and KA were selected to investigate the binding to bovine serum albumin (BSA) using UV–Vis spectroscopy, fluorescence, synchronous fluorescence, and circular dichroism (CD) at pH 7.4. The results indicated that the tryptophan residues of BSA to the distance of COS/KA, COS, and KA were <8 nm, the quenching constants K_0 were decreased, and the value of Kq were much $>2.0 \times 10^{10}$ L mol^{-1} s^{-1} for COS/KA–BSA, COS–BSA, and KA–BSA at 298, 302, 306, 310 K, respectively, those confirmed that the quenching process belongs to static quenching. The thermodynamic parameters $\Delta H°$, $\Delta G°$, $\Delta S°$ at different temperatures were calculated and indicated that hydrophobic and electrostatic forces played important roles in the binding process, and the enhanced binding affinity mainly associated with the increase of the hydrophobicity. Moreover, the CD data demonstrated that the secondary structure of BSA was slightly altered in the presence of COS/KA, COS, and KA, with different reduced α-helix contents (46.30 ± 0.20, 48.60 ± 0.40, 50.70 ± 0.20), respectively. The work provides basic data for the binding mechanism of COS/KA with BSA in vitro.

Keywords Chitosan oligosaccharides · Bovine serum albumin · Fluorescence · Circular dichroism

X. Liu · W. Xia (✉) · Q. Jiang · Y. Xu · P. Yu
State Key Laboratory of Food Science and Technology, School of Food Science and Technology, Jiangnan University, Lihu Road 1800, Wuxi 214122, Jiangsu, People's Republic of China
e-mail: xiaws@jiangnan.edu.cn

Introduction

The microbial contamination problem in food safety is a vital concern to public health, which can lead to spoilage and deteriorate the quality of food products [1] or cause infection and illness [2]. Thus, controlling pathogens could reduce foodborne outbreaks and assure consumers a safe, wholesome, and nutritious food supply [3]. Even though a large number of antimicrobials have been developed over the years, the development of antimicrobial resistance and the relatively narrow spectrum of the antimicrobials have led to limited success in controlling foodborne pathogens and the microbial contamination of food still poses important public health and economic concern for the society at large [4]. Consequently, it is necessary to find a novel way to reduce or eliminate food-related microorganisms during the shelf life of food products.

Chitosan oligosaccharides (COS) is a mixture of oligomers of β-1,4-linked D-glucosamine residues that have better biocompatibility and solubility due to its shorter chain lengths and free amino groups in D-glucosamine units. It is of special interest in agriculture, food industry, and medicine for it has activities such as elicitors of plant defense [5], antibacterial [6], antiinflammatory activity [7], and antitumour agent [8]. Meanwhile, kojic acid (KA) is widely used as a food additive for preventing enzymatic browning of shrimps [9], antimicrobial, and antiviral activities [10]. For both COS and KA are good natural food preservatives for improving food quality and safety. Hence, in our previous study [11] (Fig. 1), COS/KA was prepared using the selective partial alkylation of N-benzylidene COS and chlorokojic acid in the presence of dimethyl sulfoxide (DMSO) and pyridine (Py). The antibacterial activity results of COS/KA showed that it could inhibit the growth of damaging agents as *Staphylococcus aureus*, *Escherichia coli*, *Aspergillus niger* and *Saccharomyces cerevisiae*. In

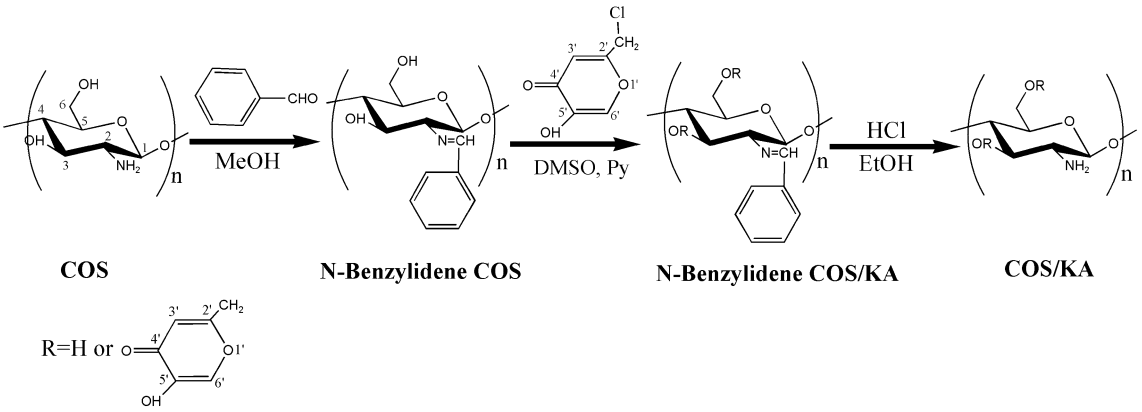

Fig. 1 Reaction scheme for the synthesis of COS/KA

addition, it exhibited an excellent solubility in organic solvents and distilled water. These characteristics could make it a novel potential antibacterial agent in food industry.

Antibacterial agents exert the pharmaceutical effects by the interaction between antibacterial agents and target cells. Often, binding of antibacterial agents to a cell membrane may result in the exposure of previously buried hydrophobic regions and the distortions of the bilayer structure and changes in the fluidity of the cell membrane. Thereby, antibacterial agents exert the antibacterial effects. Characteristics of antibacterial agents moving across cell membrane often depend on their hydrophobicity and structures [12]. Water-soluble molecules such as proteins are assisted by translocon, or by formation of α-helices and β-barrels [13].

However, up to now, the influence of COS and KA on their binding characteristics with BSA has not yet been reported, and the exact mechanism of the antimicrobial action of COS/KA is still unknown. Hence, it is important to make clear the interactive means between COS/KA and membrane protein or lipid of bacteria. Thus, as part of our ongoing investigation of antimicrobial activity of COS/KA, we simulated the effect of COS/KA, COS, and KA on BSA in vitro under physiological conditions and the conformation of membrane protein by spectroscopic methods. The study provides a quantitative understanding of the effect of COS derivatives and COS on the structure of BSA, which could be a useful supports for the further design of much more suitable COS derivatives with structural variants.

Materials and methods

Materials

Chitosan oligosaccharide (MW = 1 kDa), with a degree of deacetylation of 90 %, was made from crab shell and obtained from Zhejiang Jinke Biochemical Co. Ltd. (Zhejiang, China). Kojic acid (2-hydroxymethyl-5-hydroxy-*4H*-pyran-4-one) was purchased from Wuhan Weisheng Biochemical Co. Ltd. (Hubei, China).

Chitosan oligosaccharides–kojic acid graft copolymer (COS/KA) was prepared according to our previous method [5]. To confirm successful synthesis, ^{1}H NMR analysis was conducted. Unmodified COS: ^{1}H NMR (400 MHz, D_2O) δ: 4.5 (1H, H-1), 2.51 (2H, H–Ac), 3.24-3.94 (1H, H-2/6), 4.7 (D_2O). 1.98 ($-CH_3$). COS/KA: ^{1}H NMR (400 MHz, D_2O): a signal of newly formed three resonance signals appeared at δ: 4.19 ($-CH_2$), 6.59 (H-3') and 8.07 (H-6'). The signals of COS protons at 1.98, 2.98, and from 3.24 to 3.94 ppm did not change significantly their chemical shifts. It showed that the alkylation reaction took place at the C-6 and (or) C-3 position of COS, and the 5-hydroxypyranone group of KA was introduced to the chain of COS.

In this study, the sample with a degree of substitution (DS) 1.21 was chosen for its superior antibacterial activity. BSA (being electrophoresis-grade reagent, was obtained from Sigma) was used. The samples were dissolved in Tris–HCl buffer solution (0.05 mol L^{-1} Tris, 0.10 mol L^{-1} NaCl, pH = 7.4). All reagents were of analytical reagent grade, and doubly distilled water was used throughout the experiment.

UV–visible absorption measurements

The UV–Vis absorption spectra of solutions were obtained using a UV1000 spectrophotometer (Techcomp Ltd., China) equipped with 10 mm quartz cells in the spectral region of 190–600 nm and beam width 2 nm. The absorption spectra of BSA, COS/KA, COS, and KA their mixture were performed at room temperature.

Fluorescence measurements

All fluorescent spectra measurements were taken on an FLUORMAX-4 fluorescence spectrophotometer (HORIBA

Jobin–Yvon Co., France) quipped with a xenon lamp source and 1.0 cm quartz cells as well as an instrument of constant temperature.

To each of a series of 10-mL test tubes were successively added 1.0 mL of Tris–HCl buffer solution (pH 7.4), 1.0 mL of 1×10^{-5} mol L^{-1} BSA, and different amounts of COS/KA, COS, and KA. After equilibration for 10 min, the fluorescence spectra were then measured (excitation wavelength at 280 nm and emission wavelengths of 200–500 nm). The excitation and emission slit widths were set at 3 nm. The scan speed was 1200 nm/min. The synchronous fluorescence spectra were measured at $\lambda ex = 250$ nm and $\Delta\lambda = 60$ nm.

Circular dichroism (CD) measurements

Circular dichroism (CD) spectra were recorded over a wavelength range of 190–250 nm at 0.2-nm intervals with a scan of 50 points at 310 K in a thermostated cell holder on a MOS-450 CD spectrometer. The scanning speed was set at 200 nm/min. Results are expressed as ellipticity (mdeg), which was obtained in mdeg directly from the instrument. Three scans were made and averaged for each CD spectrum.

Statistical analyses

All experiments were carried out in triplicate, and average values with standard deviation were revealed. The data collected in this study were expressed as the mean values ±standard deviation, and significant differences between the two groups were examined using *t* test. A *P* value < 0.05 denoted the presence of a statistically significant difference (IBM SPSS Statistics 20.0, IBM, USA).

Results and discussion

UV–Vis absorption spectra

UV–Vis absorption measurement is a very simple method and applicable to explore the structural change and to know the complex formation [14]. To explore the structural change of BSA by addition of COS/KA, KA, and COS, we measured UV–Vis spectra of BSA with various amounts of the above three bacteriostatic agents [c(COS/KA) = c(COS) = c(KA)/(10^{-5} mol L^{-1}); 1 → 7: 0, 0.25, 0.5, 0.75, 1, 1.25, 1.5] (Fig. 2). In the UV–Vis spectra of them, broad absorption bands between 200 and 320 nm were observed for all the samples. Based on the data reported in the published literature, we known that BSA has two absorption peaks. The strong absorption peak at about 208 nm reflects the framework conformation of the protein, and the weak absorption peak at about 279 nm appears to be due to π → π* transition of aromatic

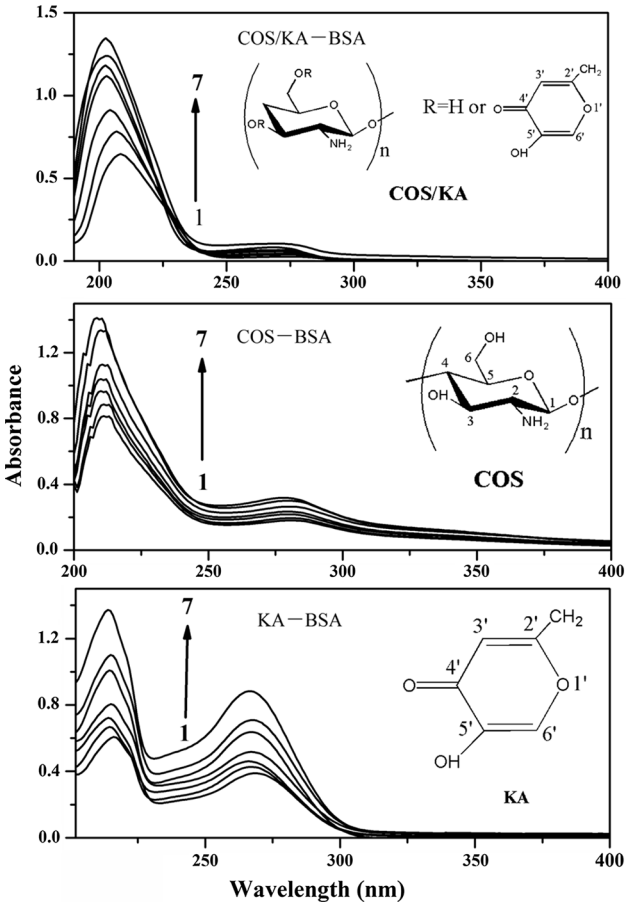

Fig. 2 UV–Vis absorption spectra of BSA in the presence of various concentrations of bacteriostatic agents 1 → 7, c (BSA) = 1×10^{-5} mol L^{-1}; c(COS/KA) = c(COS) = c(KA)/(10^{-5} mol L^{-1}); 1 → 7: 0, 0.25, 0.5, 0.75, 1, 1.25, 1.5; pH 7.4, $T = 298$ K

amino acid residues (tryptophan and tyrosine) [15–17]. In addition, it is clear from the figure that in the UV–Visible region, the absorbance of system increased with increasing concentration of the bacteriostatic agents. The intensity of the peak at 208 and 279 nm decreased, and the absorption peaks of these solutions showed moderate shifts toward shorter wave lengths in λ_{max} value by 2–5 nm indicating that with the addition of bacteriostatic agents. The above observations can be rationalized in terms of interactions between COS/KA, KA, and COS and BSA in the ground state and formation of a ground state complex. COS/KA, KA, and COS can induce the protein peptide chain extension of BSA molecules and expose the aromatic heterocyclic hydrophobic groups of tryptophan and tyrosine residues which surrounded in BSA molecules [18].

Quenching mechanism analysis

Synchronous fluorescence spectroscopy can give information about the molecular environment in the vicinity of

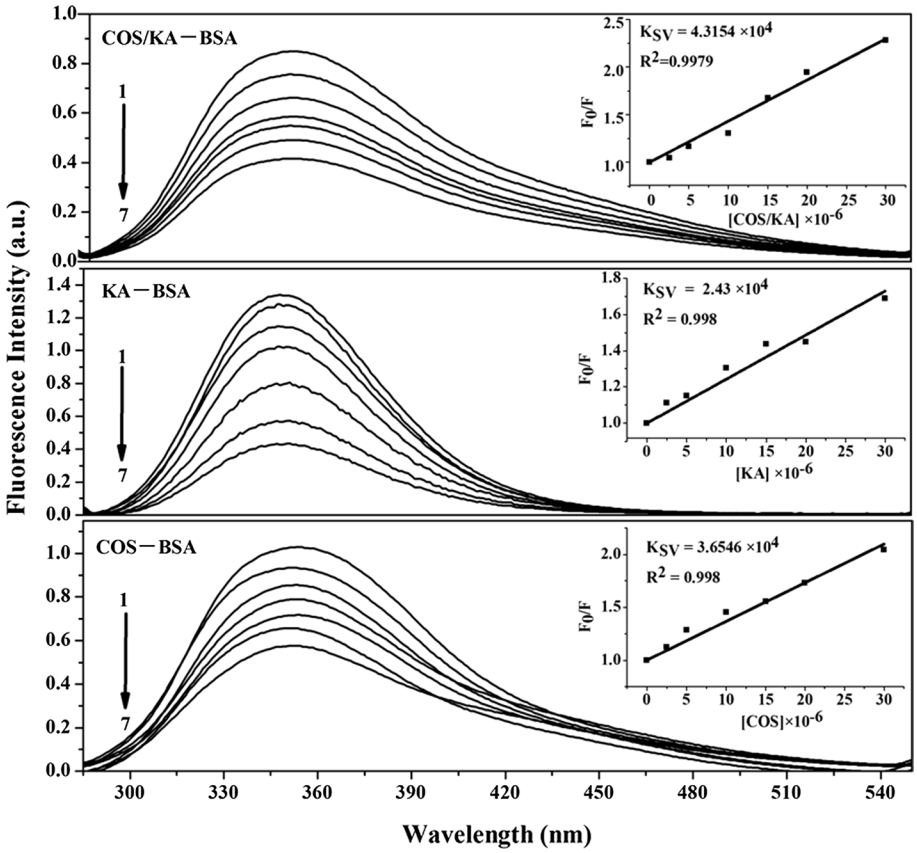

Fig. 3 Fluorescence spectra of BAS (1×10^{-5} mol L^{-1}) with COS/KA, COS, and KA (0, 0.1, 0.2, 0.4, 0.6, 0.8, 1 mg L^{-1}); pH 7.4, T = 298 K

chromophores [19] and can also give some information about the binding properties of small-molecule substances to protein, such as the binding mechanism, binding mode, binding constant, binding sites, and intermolecular distances. There are only three intrinsic fluorophores: tryptophan, tyrosine, and phenylalanine in BSA [20].

The change of intrinsic fluorescence intensity of BSA is that of fluorescence intensity of the tryptophan residue when small-molecule substances are added to BSA [21]. BSA is considered to possess intrinsic fluorescence originating from the Trp-134 and Trp-212 tryptophan residues. Trp-212 is situated within a hydrophobic binding pocket of the protein, which is in a well characterized binding cavity for small-charged aromatic molecules, while Trp-134 is thought to be located on the surface of the molecule [22].

The fluorescence spectrums of BSA quenched by COS/KA, COS, and KA at different concentrations (0, 0.1, 0.2, 0.4, 0.6, 0.8, 1 mg L^{-1}) are shown in Fig. 3. The concentrations of BSA were stabilized at 1×10^{-5} mol L^{-1}, and the content of COS/KA, COS, and KA varied from 0 to 1.5 mg mL^{-1} at the step of 0.25 mg mL^{-1}. The intensity of fluorescence can be decreased by a wide variety of processes. Such decreases in intensity are called quenching [23]. It is apparent from Fig. 3, the addition of increasing concentrations of COS/KA, COS, and KA caused a progressive reduction in the fluorescence intensity. It is noted that complex was formed between bacteriostatic agents and BSA, which is responsible for the quenching of BSA. Fluorescence peak position and peak shape of COS/KA–BSA at different concentrations are similar to COS–BSA and KA–BSA. Furthermore, a small blue shift was observed with increasing COS/KA and COS concentration, which are probably attributed to tyrosine and tryptophan residues (Trp-212 or Trp-134) of BSA [24, 25] and suggests that the fluorescence chromophore of BSA was placed in a more hydrophobic environment after the addition of COS/KA and COS. The drop of fluorescence can be rationalized by the conformational changes of BSA after the binding, which can lead to the gradual exposure of tryptophan residues to water.

Quenching mechanisms include static and dynamic quenching. To elucidate further the quenching mechanism of BSA induced by COS/KA, COS, and KA, the fluorescence quenching data are analyzed with the Stern–Volmer equation (Eq. 1) [26, 27]:

$$F_0/F = (K_q \tau_0)[Q] = 1 + K_{SV}[Q] \quad (1)$$

where F_0 and F are the fluorescence intensities before and after the addition of the quencher, respectively. Kq, K_{SV}, τ_0, and [Q] are the quenching rate constant of the bimolecular, the Stern–Volmer dynamic quenching constant, the average lifetime of the bimolecular without quencher ($\tau_0 = 10^{-8}$s),

Table 1 Binding and quenching constants according to Stern–Volmer curves

pH	T(K)		$K_{SV} \pm$ SD ($\times 10^4$ L mol^{-1})	$K_q \pm$ SD ($\times 10^{12}$ L mol^{-1}s^{-1})	R
7.4	298	COS/KA–BSA	4.32 ± 0.029^{c}	4.32 ± 0.016^{f}	0.998
		COS–BSA	3.65 ± 0.032^{b}	3.65 ± 0.033^{e}	0.998
		KA–BSA	2.43 ± 0.013^{a}	2.43 ± 0.048^{d}	0.998

R is the correlation coefficient

SD is the standard deviation (average of triplicate)

Values with different superscript letters are significantly different ($P < 0.05$); Values with the same superscript letters are not significantly different ($P > 0.05$)

Table 2 Binding constants and relative thermodynamic parameters of the COS/KA–BSA, COS–BSA, and KA–BSA system

	T (K)	ΔH° (kJ mol^{-1})	ΔS° (Jmol^{-1}K^{-1})	ΔG° (kJ mol^{-1})	$K_0 \pm$ SD (L mol^{-1})	R	$n \pm$ SD
COS/KA–BSA	298	−4.02	75.28	−26.46	$2.61 \times 10^7 \pm 0.019^{dB}$	0.993	1.53 ± 0.011^{aB}
	302			−26.76	$2.43 \times 10^7 \pm 0.013^{bcB}$	0.993	1.62 ± 0.013^{bB}
	306			−27.06	$2.36 \times 10^7 \pm 0.029^{bB}$	0.994	1.67 ± 0.009^{cB}
	310			−27.36	$2.18 \times 10^7 \pm 0.012^{aB}$	0.995	1.70 ± 0.012^{cdB}
COS–BSA	298	−10.42	52.37	−26.03	$6.88 \times 10^3 \pm 0.029^{dA}$	0.995	0.81 ± 0.008^{aA}
	302			−26.24	$6.64 \times 10^3 \pm 0.01^{bcA}$	0.997	0.87 ± 0.015^{bA}
	306			−26.44	$6.57 \times 10^3 \pm 0.009^{bA}$	0.998	0.92 ± 0.014^{cA}
	310			−26.65	$6.23 \times 10^3 \pm 0.021^{aA}$	0.992	0.96 ± 0.005^{dA}
KA–BSA	298	-12.64	41.54	−25.02	$1.81 \times 10^3 \pm 0.034^{cdA}$	0.992	0.75 ± 0.016^{aA}
	302			−25.18	$1.72 \times 10^3 \pm 0.025^{bcA}$	0.994	0.83 ± 0.014^{bA}
	306			−25.35	$1.65 \times 10^3 \pm 0.026^{bA}$	0.997	0.89 ± 0.018^{cA}
	310			−25.52	$1.48 \times 10^3 \pm 0.017^{aA}$	0.992	0.90 ± 0.017^{cA}

R is the correlation coefficient

SD is the standard deviation (average of triplicate)

Values with different superscript letters are significantly different ($P < 0.05$); Values with the same superscript letters are not significantly different ($P > 0.05$)

The superscript with lowercase letter is the significant between different temperature for COS/KA–BSA, COS–BSA, and KA–BSA. The superscript with capital letter is the significant between COS/KA–BSA, COS–BSA, and KA–BSA at the same temperature

and the concentration of the quencher, respectively. Hence, Eq. (1) was applied to determine K_{SV} by linear regression of a plot of F_0/F against [Q]. The inset in Fig. 3 shows that COS/KA, COS, and KA are found to lead to a similar fluorescence quenching within the investigated concentrations range, and the results agree with the Stern–Volmer Eq. (1). However, the extinction of BSA tryptophans by COS/KA decreases more rapidly than those caused by COS and KA. Moreover, from the slopes of the curves, it can also be concluded that the binding affinity of COS/KA to BSA is much stronger than that of KA. The Stern–Volmer plot does not show deviation toward the y-axis obviously at the experimental concentration range, which is an indication that either dynamic quenching or static quenching is predominant. Linear fittings (in Fig. 3) of the experimental data obtained afford K_{SV} and kq (Table 1). For dynamic quenching, the maximum scattering collision quenching constant of various quenchers is 2.0×10^{10} L mol^{-1}s^{-1} [26, 28]. The results showed that the value of kq was much $>2.0 \times 10^{10}$ L mol^{-1}s^{-1}, which indicates that the fluorescence quenching mechanism may be static. The quenching constants K_0 at three temperatures are found to decrease as the temperature rises which presented in Table 2. The data again confirm that the quenching process between BSA and bacteriostatic agent belongs to static quenching. Hence, the probable quenching mechanism of fluorescence of BSA by COS/KA, COS, and KA is not caused dynamic collision but from the formation of a complex.

Binding constant and number of binding sites

For the static quenching interaction, when small molecules bind independently to a set of equivalent sites on a macromolecule, the binding constant (K_0) and the number of binding sites (n) can be determined by the equation [29]:

$$\lg[(F_0 - F)/F] \lg K_0 + n \lg[Q] \quad (2)$$

Where F_0, F, and [Q] are the same as in Eq. (1), K_0 and n are the binding constant and the number of binding sites, respectively. Plots of log $(F_0 - F)$/F versus log $[Q]$ of the fluorescence quenching of BSA with different concentrations of COS/KA, COS, and KA are shown in Fig. 4. The values of binding constant K_0 and the number of binding sites per BSA are listed in Table 2. The values of K_0 suggest that there is a strong binding force between COS/KA, COS and BSA. It can be inferred from the values of n that there is about one independent class of binding sites on BSA for the ligand. The larger K_0 implies the increased stability of the BSA-bacteriostatic agent complex, which suggests that the addition of KA has effects on the interactions between COS and BSA. The linear quotieties are larger than 0.99, and the standard deviation is <0.05, indicating that the assumptions underlying the derivation of Eq. (2) are satisfied. The values of n approximately equal to 1 indicate the existence of just a single binding site in BSA for COS/KA during their interaction.

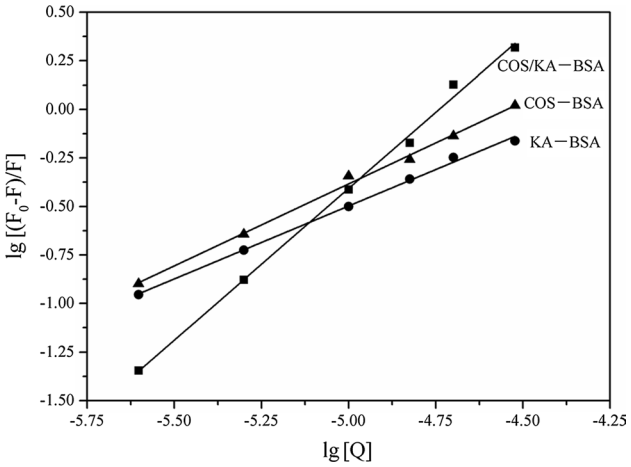

Fig. 4 Logarithmic plot of the fluorescence quenching of BSA with different concentrations of COS/KA, COS, and KA

Thermodynamic parameters and nature of the binding forces

There are essentially four types of noncovalent interactions that could play a role in ligand binding to proteins. These are hydrogen bonds, van der Waals forces, electrostatic, and hydrophobic interactions [30]. To obtain such information, the implications of the present results have been discussed in conjunction with thermodynamic characteristics obtained for hesperidin binding, and the thermodynamic parameters were calculated from the Van't Hoff equation. The slope of a plot of the bimolecular quenching constant versus 1/T (T, absolute temperature) allows one to calculate the energy change for the quenching process [15]. If the enthalpy change ΔH° does not vary significantly over the temperature range studied, then its value and that of entropy change ΔS° can be determined from the Van't Hoff equation:

$$\text{In K} = -\frac{\Delta H}{RT} + \frac{\Delta S}{R} \tag{3}$$

where K is the Stern–Volmer quenching constant at the corresponding temperature and R is the gas constant. The temperatures used were 298, 302, 306 and 310 K. The enthalpy change ΔH° and entropy change ΔS° were obtained from the slope and intercept of the linear Van't Hoff plot (Fig. 5) of lnK versus 1/T based on Eq. (3). The free energy change ΔG° is estimated from the following relationship:

$$\Delta G^0 = \Delta H^0 - T\Delta S \tag{4}$$

Table 2 shows the values of ΔH° and ΔS° obtained for the binding site from the slopes and ordinates at the origin of the fitted lines.

From Table 2, it can be seen that the negative sign for free energy ΔG° means that the interaction process is

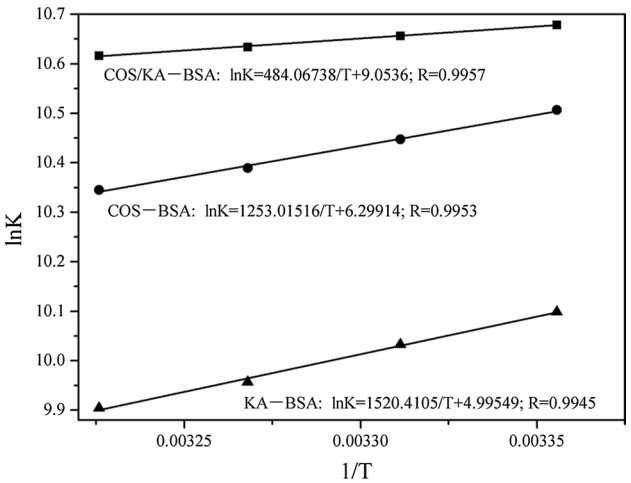

Fig. 5 Van't Hoff plot, pH 7.40, c(BSA) = 1.0×10^{-5} mol L^{-1}

spontaneous. ΔH° is a small negative value, and ΔS° is a positive value. It is indicated that electrostatic forces play the major role during the interaction (COS and KA). Because under the experimental conditions used the pH (7.4) is much greater than the isoelectric point of BSA (4.7), BSA is negatively charged, COS is also negatively charged, and KA is positively charged at pH 7.4. Although BSA and COS are both negatively charged, COS can interact with the positively charged amino acid residues of BSA through electrostatic forces. The main source of ΔG° value is derived from a large contribution of ΔS° term with little contribution from the ΔH° factor. From the point of view of water structure, a positive ΔS° value is frequently taken as evidence for hydrophobic interaction. Furthermore, specific electrostatic interactions between ionic species in aqueous solution are characterized by a positive value of

(ΔS°) and a negative ΔH°. Accordingly, it is not possible to account for the thermodynamic parameters of COS/KA–BSA coordination compound on the basis of a single intermolecular force model [30]. It is more likely hydrophobic, electrostatic interactions are involved in its binding process. Hence, it can be concluded that COS/KA has the strongest affinity to BSA and the binding of KA to BSA was weaker than that of COS. This conclusion is compatible with the results obtained by comparing the binding constant values of the three compounds to BSA.

Energy transfer between bacteriostatic agents and BSA

In order to further confirm the binding feature of bacteriostatic agents–BSA system, the binding distances (r) between the acceptor (COS/KA, COS, and KA) and the donor (BSA) were determined by Förster's theory of dipole energy transfer [23]. The Förster theory of molecular resonance energy transfer points out: In addition to radiation and reabsorption, a transfer of energy could also take place through direct electrodynamic interaction between the primarily excited molecule and its neighbors. According to this theory, the distance of binding between bacteriostatic agents and BSA could be calculated by the equation [31]:

$$E = 1 - \frac{F}{F_0} = \frac{R_0^6}{R_0^6 + r_0^6} \tag{5}$$

In Eq. (5), r is the distance between the donor and acceptor and R_0 is the critical distance when the transfer efficiency is 50 %, which can be calculated by the equation:

$$R_0^6 = 8.79 \times 10^{-25} K^2 n^{-4} \phi J \tag{6}$$

In Eq. (6), K^2 is a factor describing the relative orientation in space of the transition dipoles of the donor and acceptor, n is the refractive index of the medium, Φ is the fluorescence quantum yield of the donor in the absence of acceptor and the overlap integral J expresses the degree of spectral overlap between the donor emission and the acceptor absorption. J can be given by.

$$J = \frac{\int_0^\infty F(\lambda)\varepsilon(\lambda)\lambda^4 d\lambda}{\int_0^\infty F(\lambda) d\lambda} \tag{7}$$

where F (λ) is the fluorescence intensity of the fluorescent donor at wavelength λ and ε (λ) is the molar absorptive of the acceptor at wavelength λ.

Here, the donor and acceptor were BSA and the above three bacteriostatic agents, respectively.

The overlap of the absorption spectrum of bacteriostatic agents and the fluorescence emission spectrum of BSA is shown in Fig. 6. J can be evaluated by integrating the spectra according to Eq. (7). For BSA, $K^2 = 2/3$, $n = 1.336$, and $\Phi = 0.15$ [32]. A transfer of energy could take place through direct electrodynamic interaction between the primarily excited molecule and its neighbors, with an important condition: the distance between the donor and the acceptor is approach in the range of 2–8 nm [33]. All the results are shown in Table 3. The donor (tryptophan residues of the BSA) to acceptor (COS/KA, COS, KA) distance was <8 nm, these accord with conditions of Forster's nonradiative energy transfer theory, indicating the fluorescence quenching of BSA is also a nonradiation transfer process [34]. The different values of r imply the different degrees of conformational changes of BSA induced by the three compounds, although they bind the similar site on BSA.

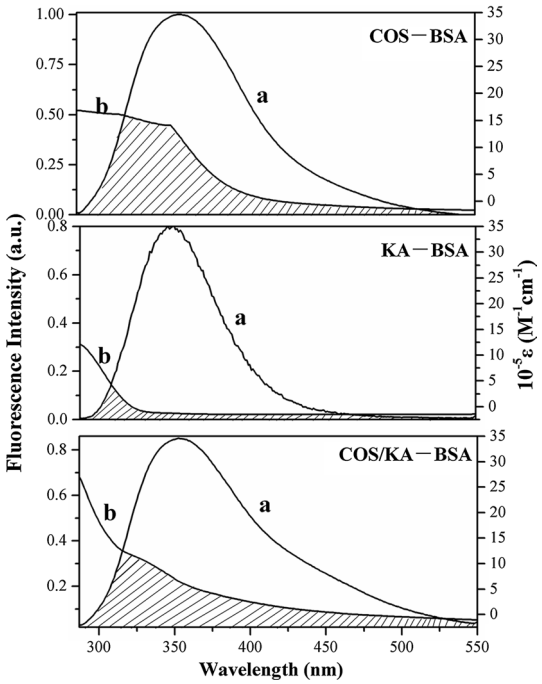

Fig. 6 Spectral overlap of COS/KA, COS, and KA absorption with BSA fluorescence, c(COS/KA) = c(COS) = c(KA) = c(BSA) = 1.0 × 10^{-5} mol L^{-1}; pH 7.4, T = 298 K

Table 3 The calculated J, E and r values of COS/KA–BSA, COS–BSA, and KA–BSA

	J (cm^3 L mol^{-1})	E (%)	R_0 (nm)	r (nm)
COS/KA–BSA	2.88 × 10^{-14}	28.50	2.22	3.26
COS–BSA	2.76 × 10^{-14}	26.70	2.18	3.23
KA–BSA	2.13 × 10^{-14}	28.00	2.16	3.25

Synchronous fluorescence spectroscopic studies

Synchronous fluorescence spectroscopy is a very useful method to study the microenvironment of amino acid residues by measuring the emission wavelength shift [35], and

it can provide the information about the molecular environment in the vicinity of the chromophore molecules. In the synchronous spectra, the sensitivity associated with fluorescence is maintained while offering several advantages: spectral simplification, spectral bandwidth reduction, and avoiding different perturbing effects [23]. When the D-value ($\Delta\lambda$) between excitation wavelength and emission wavelength are stabilized at 15 or 60 nm, the synchronous fluorescence gives the characteristic information of tyrosine or tryptophan residues. The synchronous fluorescence spectra of BSA with various amounts of COS/KA, COS, and KA (c(COS/KA) = c(COS) = c(KA)/(10^{-5} mol L^{-1}); 1 → 7: 0, 0.25, 0.5, 0.75, 1, 1.25, 1.5) were recorded at $\Delta\lambda$ = 60 nm (Fig. 7). The intrinsic fluorophores in serum albumins show significant advantages, because tryptophan is highly sensitive to the local environment and also displays a substantial spectral shift.

The emission wavelength of the tryptophan residues is blue-shifted (λ_{max}: 285–282, 286–283, 284–279 nm) with increasing concentration of COS/KA, COS, and KA. The blue-shifted effect express the conformation of BSA was changed. It is also indicated that the polarity around the tryptophan residues was decreased and the hydrophobicity was increased, which was in accordance with the result obtained from UV–visible spectroscopy technique mentioned above. At the same time, the tyrosine fluorescence emission ($\Delta\lambda$ = 15 nm) is decreased regularly, but no significant change in wavelength was observed (date not shown). It suggests that the interaction of COS/KA, COS, and KA with BSA does not affect the conformation of tyrosine microregion.

Secondary structural changes of BSA shown by CD

Circular dichroism (CD) is a relative powerful technique to investigate the secondary structural change of proteins, because they are, in the far ultraviolet region, related to the polypeptide backbone structure of proteins. To gain a better understanding in bacteriostatic agents–protein binding mechanism and secondary structure changes of protein, additional CD measurements were taken on BSA and bacteriostatic agents–BSA complex. Figure 8 shows the CD spectra of BSA with various amounts of bacteriostatic agents [c (BSA) = c (COS/KA) = c (COS) = c (KA) = 1.0 × 10^{-5} mol L^{-1}] at pH 7.4. The CD spectra of BSA are characterized mainly by two negative bands at 208 and 222 nm, which are rationalized by the n → π* transition in the peptide bond of α-helical [36]. It was observed from Fig. 8 that there was an obvious reduction in both of these bands without any significant shift of the peaks in the presence of COS/KA, COS, and KA, indicating the decrease of α-helical content in protein. The decrease of α-helix content indicates that the binding of COS/KA, COS, and KA with BSA induces some conformational changes in BSA, which may affect the physiological functions of BSA. The influence of COS/KA, COS, and KA on

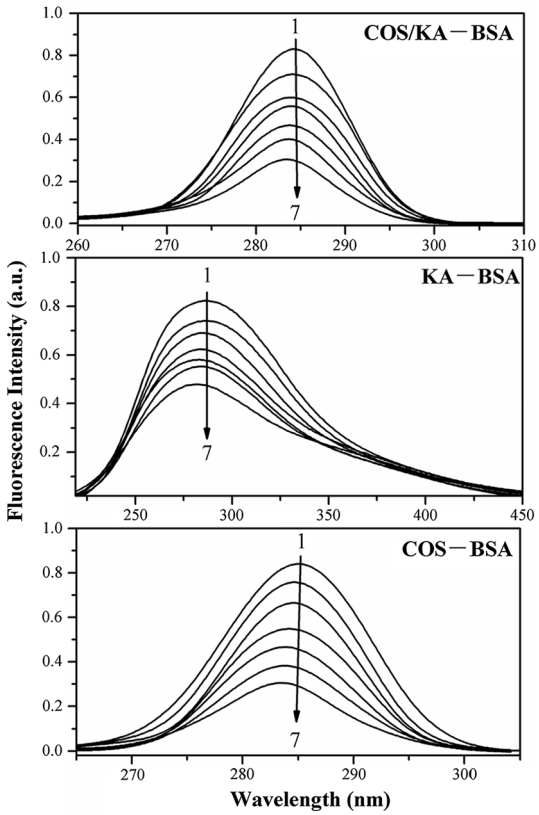

Fig. 7 Synchronous fluorescence spectrum of BSA: $\Delta\lambda$ = 60 nm, c(BSA) = 1.0 × 10^{-5} mol L^{-1}; c(COS/KA) = c(COS) = c(KA)/(10^{-5} mol L^{-1}); 1 → 7: 0, 0.25, 0.5, 0.75, 1, 1.25, 1.5; pH 7.4, T = 298 K

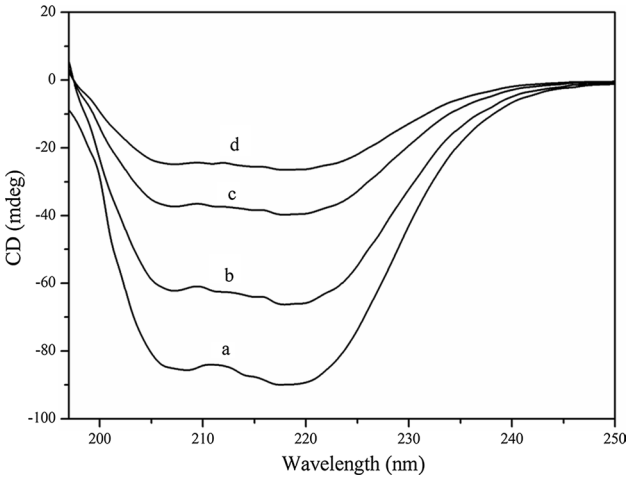

Fig. 8 CD spectra of BSA and COS/KA–BSA, COS–BSA, and KA–BSA system. Conditions: c(BSA) = c(COS/KA) = c(COS) = c(KA) = 1.0 × 10^{-5} mol L^{-1}; *a* BSA, *b* COS/KA–BSA, *c* COS–BSA, *d* KA–BSA system; pH 7.4, T = 298 K

Table 4 Influence of COS/KA, COS, and KA on the secondary structure element of BSA

System	α-Helix (%)	β-Sheet (%)	β-Turn (%)	Random (%)
Pure BSA	51.80 ± 0.50^{cd}	15.10 ± 0.20^{a}	5.30 ± 0.20^{a}	27.80 ± 0.50^{bc}
COS/KA–BSA	46.30 ± 0.20^{a}	18.70 ± 0.30^{d}	7.90 ± 0.30^{c}	27.10 ± 0.20^{a}
COS–BSA	48.60 ± 0.40^{b}	17.30 ± 0.40^{c}	6.50 ± 0.20^{b}	27.60 ± 0.20^{bc}
KA–BSA	50.70 ± 0.20^{c}	15.80 ± 0.30^{ab}	6.10 ± 0.40^{b}	27.40 ± 0.40^{b}

SD is the standard deviation (average of triplicate)

Values with different superscript letters are significantly different ($P < 0.05$); Values with the same superscript letters are not significantly different ($P > 0.05$)

the secondary structure element of BSA was presented in Table 4. With the addition of COS/KA, COS, and KA to BSA (1:1), the β-sheet increased from 15.1 % in free BSA to 18.7, 17.3, and 15.8 %, respectively, while the β-turn increased from 5.3 % in free BSA to 7.9, 6.5, and 6.1 %, respectively.

On the other hand, it is also seen from the data that the binding of COS/KA, COS, and KA with BSA causes obvious conformational change, but the degree of change in conformation of BSA on the binding of COS/KA is a little greater than on the binding of COS and KA. That is to say, the effect of COS/KA on the conformation of BSA is a little more pronounced than COS and KA.

As mentioned above, the binding of COS/KA, COS, and KA can lead to the loosening and unfolding of the protein skeleton and increases the hydrophobicity of the microenvironment of the tryptophan residues of BSA. These results are in agreement with those obtained from UV–visible spectroscopy technique mentioned above.

Conclusions

In this paper, the binding properties of COS/KA, COS, and KA to BSA were characterized by measuring the UV–Vis spectroscopy, fluorescence spectroscopy, synchronous fluorescence, and circular dichroism (CD). The results reveal that the introduction of 5-hydroxypyranone group of KA by alkylation reaction at positions C3 and (or) C6 of COS can influence the binding characteristics of COS derivatives to BSA and the binding affinity follows the order: COS/KA > COS > KA. COS/KA, COS, and KA displayed static quenching on the fluorescence of BSA, which was produced by the spontaneous formation of a moderately strong complex with BSA. On the basis of the thermodynamic parameters, hydrophobic and electrostatic interactions played major roles in the binding of COS/KA, COS, and KA to BSA. In addition, COS/KA was found to bind more strongly than COS and KA. Furthermore, the results of CD spectrum indicate that the secondary structure of BSA molecules is changed in the presence of COS/KA, COS, and KA. These results demonstrate that the introduction of 5-hydroxypyranone group to COS chain has a profound impact on its binding affinity with BSA. The work provides basic data for the binding mechanism of COS/KA with BSA in vitro.

Acknowledgments We thank the staff at our laboratory for the assistance they have provided in this study. This research was financially supported by the Twelfth Five Year National Science and Technology Plan of rural field research mission contract (2011BAD23B00), and the Fund Project for Transformation of Scientific and Technological Achievements of Jiangsu Province (BA2009082).

Conflict of interest None.

Compliance with Ethics Requirements This article does not contain any studies with human or animal subjects.

References

1. Celiktas OY, Kocabas E, Bedir E, Sukan FV, Ozek T, Baser K (2007) Antimicrobial activities of methanol extracts and essential oils of Rosmarinus officinalis, depending on location and seasonal variations. Food Chem 100(2):553–559. doi:10.1016/j.foodchem.2005.10.011
2. Jacob C, Mathiasen L, Powell D (2010) Designing effective messages for microbial food safety hazards. Food Control 21(1):1–6. doi:10.1016/j.foodcont.2009.04.011
3. Kim J, Marshall MR, Wei C-i (1995) Antibacterial activity of some essential oil components against five foodborne pathogens. J Agric Food Chem 43(11):2839–2845. doi:10.1021/jf00059a013
4. Vattem DA, Lin YT, Labbe RG, Shetty K (2004) Phenolic antioxidant mobilization in cranberry pomace by solid-state bioprocessing using food grade fungus Lentinus edodes and effect on antimicrobial activity against select food borne pathogens. Innov Food Sci Emerg Technol 5(1):81–91. doi:10.1016/j.ifset.2003.09.002
5. Cho Y-S, Lee S-H, Kim S-K, Ahn C-B, Je J-Y (2011) Aminoethylchitosan inhibits LPS-induced inflammatory mediators, iNOS and COX-2 expression in RAW264. 7 mouse macrophages. Process Biochem 46(2):465–470. doi:10.1016/j.procbio.2010.09.019
6. Jeon Y-J, Kim S-K (2000) Production of chitooligosaccharides using an ultrafiltration membrane reactor and their antibacterial activity. Carbohydr Polym 41(2):133–141. doi:10.1016/S0144-8617(99)00084-3
7. Xia W, Liu P, Zhang J, Chen J (2011) Biological activities of chitosan and chitooligosaccharides. Food Hydrocolloids 25(2):170–179. doi:10.1016/j.foodhyd.2010.03.003

8. Qin C, Zhou B, Zeng L, Zhang Z, Liu Y, Du Y, Xiao L (2004) The physicochemical properties and antitumor activity of cellulase-treated chitosan. Food Chem 84(1):107–115. doi:10.1016/S0308-8146(03)00181-X
9. Chen JS, Wei C-I, Rolle RS, Otwell WS, Balaban MO, Marshall MR (1991) Inhibitory effect of kojic acid on some plant and crustacean polyphenol oxidases. J Agric Food Chem 39(8):1396–1401. doi:10.1021/jf00008a008
10. Aytemir MD, Özçelik B (2010) A study of cytotoxicity of novel chlorokojic acid derivatives with their antimicrobial and antiviral activities. Eur J Med Chem 45(9):4089–4095. doi:10.1016/j.ejmech.2010.05.069
11. Liu X, Xia W, Jiang Q, Xu Y, Yu P (2013) Synthesis, characterization, and antimicrobial activity of kojic acid grafted chitosan oligosaccharide. J Agric Food Chem 62(1):297–303. doi:10.1021/jf404026f
12. Giess F, Friedrich MG, Heberle J, Naumann RL, Knoll W (2004) The Protein-Tethered Lipid Bilayer: a Novel Mimic of the Biological Membrane. Biophys J 87(5):3213–3220. doi:10.1529/biophysj.104.046169
13. Parker M, Pattus F, Tucker A, Tsernoglou D (1989) Structure of the membrane-pore-forming fragment of colicin A. Nature 337:93–96. doi:10.1038/337093a0
14. Bi S, Song D, Kan Y, Xu D, Tian Y, Zhou X, Zhang H (2005) Spectroscopic characterization of effective components anthraquinones in Chinese medicinal herbs binding with serum albumins. Spectrochim Acta Part A Mol Biomol Spectrosc 62(1):203–212. doi:10.1016/j.saa.2004.12.049
15. Ravindran A, Singh A, Raichur AM, Chandrasekaran N, Mukherjee A (2010) Studies on interaction of colloidal Ag nanoparticles with bovine serum albumin (BSA). Colloids Surf, B 76(1):32–37. doi:10.1016/j.colsurfb.2009.10.005
16. Wang F, Huang W, Dai Z (2008) Spectroscopic investigation of the interaction between riboflavin and bovine serum albumin. J Mol Struct 875(1):509–514. doi:10.1016/j.molstruc.2007.05.034
17. Yang Q, Liang J, Han H (2009) Probing the interaction of magnetic iron oxide nanoparticles with bovine serum albumin by spectroscopic techniques. J Phys Chem B 113(30):10454–10458. doi:10.1021/jp904004w
18. Wu T, Wu Q, Guan S, Su H, Cai Z (2007) Binding of the environmental pollutant naphthol to bovine serum albumin. Biomacromolecules 8(6):1899–1906. doi:10.1021/bm061189v
19. Chi Z, Liu R, Teng Y, Fang X, Gao C (2010) Binding of oxytetracycline to bovine serum albumin: spectroscopic and molecular modeling investigations. J Agric Food Chem 58(18):10262–10269. doi:10.1021/jf101417w
20. Mote U, Bhattar S, Patil S, Kolekar G (2010) Interaction between felodipine and bovine serum albumin: fluorescence quenching study. Luminescence 25(1):1–8. doi:10.1002/bio.1130
21. Zhang G, Zhao N, Hu X, Tian J (2010) Interaction of alpinetin with bovine serum albumin: probing of the mechanism and binding site by spectroscopic methods. Spectrochim Acta Part A Mol Biomol Spectrosc 76(3):410–417. doi:10.1016/j.saa.2010.04.009
22. Bourassa P, Kanakis C, Tarantilis P, Pollissiou M, Tajmir-Riahi H (2010) Resveratrol, Genistein, and Curcumin Bind Bovine Serum Albumin†. J Phys Chem B 114(9):3348–3354. doi:10.1021/jp9115996
23. Hu Y-J, Liu Y, Wang J-B, Xiao X-H, Qu S-S (2004) Study of the interaction between monoammonium glycyrrhizinate and bovine serum albumin. J Pharm Biomed Anal 36(4):915–919. doi:10.1016/j.jpba.2004.08.021
24. Liu X-F, Xia Y-M, Fang Y (2005) Effect of metal ions on the interaction between bovine serum albumin and berberine chloride extracted from a traditional Chinese Herb coptis chinensis franch. J Inorg Biochem 99(7):1449–1457. doi:10.1016/j.jinorgbio.2005.02.025
25. Yuan T, Weljie AM, Vogel HJ (1998) Tryptophan fluorescence quenching by methionine and selenomethionine residues of calmodulin: orientation of peptide and protein binding. Biochemistry 37(9):3187–3195. doi:10.1021/bi9716579
26. Li D, Zhu J, Jin J (2007) Spectrophotometric studies on the interaction between nevadensin and lysozyme. J Photochem Photobiol, A 189(1):114–120. doi:10.1016/j.jphotochem.2007.01.017
27. Xie M-X, Long M, Liu Y, Qin C, Wang Y-D (2006) Characterization of the interaction between human serum albumin and morin. Biochimica et Biophysica Acta (BBA)-General Subjects 1760(8):1184–1191.doi: 10.1016/j.bbagen.2006.03.026
28. Ware WR (1962) Oxygen quenching of fluorescence in solution: an experimental study of the diffusion process. J Phys Chem 66(3):455–458. doi:10.1021/j100809a020
29. Xie M-X, Xu X-Y, Wang Y-D (2005) Interaction between hesperetin and human serum albumin revealed by spectroscopic methods. Biochimica et Biophysica Acta (BBA)-General Subjects 1724 (1): 215–224.doi: 10.1016/j.bbagen.2005.04.009
30. Wang Y-Q, Zhang H-M, Zhang G-C, Tao W-H, Tang S-H (2007) Interaction of the flavonoid hesperidin with bovine serum albumin: a fluorescence quenching study. J Iumin 126(1):211–218. doi:10.1016/j.jlumin.2006.06.013
31. Horrocks Jr WD, Peter Snyder A (1981) Measurement of distance between fluorescent amino acid residues and metal ion binding sites. Quantitation of energy transfer between tryptophan and terbium (III) or europium (III) in thermolysin. Biochem Biophys Res Commun 100 (1):111–117.doi: 10.1016/S0006-291X(81)80070-8
32. Kurittu J, Lönnberg S, Virta M, Karp M (2000) A group-specific microbiological test for the detection of tetracycline residues in raw milk. J Agric Food Chem 48(8):3372–3377. doi:10.1021/jf9911794
33. Li D, Zhu M, Xu C, Ji B (2011) Characterization of the baicalein–bovine serum albumin complex without or with Cu^{2+} or Fe^{3+} by spectroscopic approaches. Eur J Med Chem 46(2):588–599. doi:10.1016/j.ejmech.2010.11.038
34. Li S, Huang K, Zhong M, Guo J, Wang W-z, Zhu R (2010) Comparative studies on the interaction of caffeic acid, chlorogenic acid and ferulic acid with bovine serum albumin. Spectrochim Acta Part A Mol Biomol Spectrosc 77(3):680–686. doi:10.1016/j.saa.2010.04.026
35. Congdon RW, Muth GW, Splittgerber AG (1993) The binding interaction of Coomassie blue with proteins. Anal Biochem 213(2):407–413. doi:10.1006/abio.1993.1439
36. Lu J-Q, Jin F, Sun T-Q, Zhou X-W (2007) Multi-spectroscopic study on interaction of bovine serum albumin with lomefloxacin–copper (II) complex. Int J Biol Macromol 40(4):299–304. doi:10.1016/j.ijbiomac.2006.08.010